layer of streptavidin–Fab fragment–HCG was constructed on a desthiobiotin surface, as shown in Fig. 4, steps a through c (10 mol% **7** and 90 mol% 11-hydroxyundecylmercaptane). The addition of an excess of free biotin resulted in the competitive replacement of the entire multilayer as a result of the higher affinity of biotin to streptavidin. The restored desthiobiotin surface was used again for the reassembly of the streptavidin–Fab fragment–HCG triple layer, and the layer thickness of each of the proteins was as determined for the first triple layer. Moreover, using a single streptavidin-desthiobiotin layer, we repeated this cycle of docking and competitive replacement of streptavidin several times on the same desthiobiotin functionalized surface (*17*).

In conclusion, streptavidin matrices are versatile model systems for the tailoring of bioreactive surfaces and for the cyclic formation of protein multilayer structures. On the basis of this concept, questions concerning naturally occurring recognition processes, as well as the development of diagnostic tools such as biosensors, can be addressed. Furthermore, recognition-induced formation of organized protein–inorganic multilayers will become possible.

REFERENCES AND NOTES

1. H. J. Müller-Eberhard, *Annu. Rev. Biochem.* **57**, 321 (1988); N. R. Cooper, *Adv. Immunol.* **37**, 151 (1985).
2. M. Chaiet and F. J. Wolf, *Arch. Biochem. Biophys.* **106**, 1 (1964); N. M. Green, in *Avidin-Biotin Technology*, E. A. Bayer and M. Wilchek, Eds. (Academic Press, San Diego, CA, 1990) [*Methods Enzymol.* **184**, 51 (1990)].
3. N. M. Green, *Adv. Protein Chem.* **29**, 85 (1975).
4. R. Blankenburg, P. Meller, H. Ringsdorf, C. Salesse, *Biochemistry* **28**, 8214 (1989).
5. M. Ahlers, W. Müller, A. Reichert, H. Ringsdorf, J. Venzmer, *Angew. Chem.* **102**, 1310 (1990); *Angew. Chem. Int. Ed. Engl.* **29**, 1269 (1990).
6. S. A. Darst *et al.*, *Biophys. J.* **59**, 387 (1991).
7. W. A. Hendrickson *et al.*, *Proc. Natl. Acad. Sci. U.S.A.* **86**, 2190 (1989).
8. H. Ebato *et al.*, *Angew. Chem.* **104**, 1064 (1992); *Angew. Chem. Int. Ed. Engl.* **31**, 1078 (1992).
9. J. N. Herron *et al.*, *Langmuir* **8**, 1413 (1992).
10. M. Ahlers *et al.*, *Makromol. Chem. Macromol. Symp.* **46**, 307 (1991).
11. H. Morgan and D. M. Taylor, *Biosensors* **7**, 405 (1992).
12. R. C. Ebersole, J. A. Miller, J. R. Moran, M. D. Ward, *J. Am. Chem. Soc.* **112**, 3239 (1990).
13. The streptavidin matrix was prepared at the air-water interface as described by Blankenburg *et al.* (*4*). We then removed the excess of streptavidin by exchanging the subphase. Sulforhodamine-labeled Con A, saturated with four equivalents of biotin-sugar linker **1**, was injected underneath the streptavidin matrix and incubated for 30 min. The subphase was exchanged again to remove the excess of Con A. The third protein layer was prepared by injection of fluorescein-labeled streptavidin underneath the streptavidin–Con A double layer.
14. The liposomes were prepared by sonification of a mixed lipid film (5 mol% **3**, 95 mol% **4**) in phosphate buffer (50 mM, pH 8.5) at 60°C. We performed the ultraviolet polymerization of the diacetylene units by irradiating the suspension at 254 nm.
15. L. Häußling, B. Michel, H. Ringsdorf, H. Rohrer, *Angew. Chem.* **103**, 568 (1991); L. Häußling, W. Knoll, H. Ringsdorf, F.-J. Schmitt, J. Yang, *Makromol. Chem. Macromol. Symp.* **46**, 145 (1991).
16. J. Spinke, thesis, University of Mainz, Mainz, Germany (1992).
17. Self-assembled biotin-containing monolayers were formed on clean, vacuum-evaporated gold films. The adsorptions of the thiols were performed in ethanolic solutions with a total thiol concentration of 5×10^{-4} M (10 mol% **7**, 90 mol% 11-undecylhydroxymercaptane). All proteins were adsorbed from solutions whose concentrations were 5×10^{-7} M with respect to the proteins and 0.5 M with respect to NaCl. The adsorption processes were followed in real time by surface plasmon spectroscopy. First, streptavidin was adsorbed onto the functionalized gold, and then after the adsorption process was finished, the solution was exchanged and the biotinylated Fab fragment was adsorbed (5×10^{-7} M Fab fragment, 0.5 M NaCl) up to saturation. The solution was exchanged once again and HCG was then added. Once the triple layer formation was completed and the solution had been exchanged, biotin was added in a concentration of 2×10^{-4} M.

6 July 1993; accepted 19 October 1993

Inner Core Anisotropy Due to the Magnetic Field–Induced Preferred Orientation of Iron

Shun-ichiro Karato

Anisotropy of the inner core of the Earth is proposed to result from the lattice preferred orientation of anisotropic iron crystals during their solidification in the presence of a magnetic field. The resultant seismic anisotropy is related to the geometry of the magnetic field in the core. This hypothesis implies that the observed anisotropy (fast velocity along the rotation axis) indicates a strong toroidal field in the core, which supports a strong field model for the geodynamo if the inner core is made of hexagonal close-packed iron.

The Earth's inner core is considered to be made of solid iron (or iron-nickel alloy) (*1*). Like the silicate upper mantle, the presence of anisotropic structure has been inferred by recent seismological studies (*2*). Anisotropy appears to have axial symmetry, the fast direction being parallel to the rotation axis with an amplitude of $\sim$3% (*2*). Understanding the origin of this anisotropic structure will effect a better understanding of the dynamics of the core.

Jeanloz and Wenk (*3*) proposed that this anisotropy might be caused by the lattice preferred orientation (LPO) of iron with hexagonal close-packed (hcp) structure (ε-Fe) due to plastic deformation. Seismic anisotropy due to deformation-induced preferred orientation is well documented in the upper mantle of the Earth (*4*), but there are a number of problems in applying such a model to the inner core. First, the differential stresses in the inner core are expected to be low ($\sim 10^{-3}$ to 10^{-1} MPa) (*3*) because of the small thermal expansion, small gravity, and high thermal conductivity (Table 1). Small stresses favor diffusion or superplastic creep rather than dislocation creep for a reasonable range of grain size (*5*). Diffusion or superplastic creep produces no preferred orientation and even destroys any preexisting preferred orientation, and hence no anisotropy is expected in materials deformed by diffusion or superplastic creep (*6*). Second, and more fundamentally, even the presence of convection in the inner core can be questioned for the following reasons: (i) Heat generation due to radioactive elements in the core is likely to be low (*7*); (ii) a likely presence of gradient of oxygen content in the inner core will have a stabilizing effect against convection (*8*); and (iii) the presence of a strong magnetic field will tend to stabilize against convective instability (*9*). Third, it is not straightforward to explain the observed axial symmetry of seismic anisotropy that is based on Jeanloz and Wenk's model because there is no obvious relation between convective pattern and rotation axis. Fourth, the strength of anisotropy predicted by Jeanloz and Wenk's model is much weaker ($\sim$0.4%) than that observed ($\sim$3%) (*10*).

In this report, I propose an alternative model. This model invokes an interaction of the magnetic field with growing magnetically anisotropic iron crystals. As such, the model implies that the seismic anisotropy carries information about the geometry (and strength) of the magnetic field in the core that is not directly observable. It is shown that the observed seismic anisotropy is consistent with the strong toroidal field, but not with the weak field model of the geodynamo.

There has been a considerable debate about the likely crystal structure of iron in the inner core. Following Jephcoat and Olson (*1*) and Jeanloz (*1*), I will assume that the Earth's inner core is predominantly

---

Department of Geology and Geophysics, University of Minnesota, Minneapolis, MN 55455.

Table 1. Some physical properties of the Earth's inner core (measured in SI units). All the data except those for χ and B are from Jeanloz and Wenk (*3*). For a discussion of magnetic susceptibility, see the text. For the strength of magnetic field, see (*24*).

Property	Size
Radius (R)	1.2×10^6 m
Mean density (ρ)	1.3×10^4 kg m^{-3}
Electrical conductivity (σ)	6×10^5 S m^{-1}
Kinematic viscosity (ν)	10^9 m^2 s^{-1}*
Magnetic field (B)	10^{-3} to 10^{-2} T
Magnetic susceptibility (χ)	1×10^{-4} to 5×10^{-4}
Thermal diffusivity (κ)	1.5×10^{-5} m^2 s^{-1}
Thermal expansion (α)	7×10^{-6} K^{-1}
Acceleration of gravity (g)	0 to 4.4 m s^{-2}

*Uncertainty in the exponent is 9 ± 3.

hcp iron. However, there are some experimental and theoretical studies that suggest that a new phase might be stable at the inner core conditions, although the crystal structure of a new phase and its stability field have not been well constrained (*11*). Possible structures of a new phase include cubic structures such as face-centered-cubic (fcc) or body-centered-cubic (bcc) or a tetragonal structure. The notion of magnetic field–induced anisotropy would be applicable for any noncubic structures (*12*), although specific predictions on the nature of anisotropy depend on the assumed structure.

Hexagonal close-packed metals in general have anisotropic physical properties, including paramagnetic susceptibility (*13, 14*) and elastic wave velocities (*15*). Wenk *et al.* (*15*) reviewed the elastic anisotropy in hcp metals and concluded that the nature of elastic anisotropy is related to the crystal structure. For materials with $c/a < (c/a)_0$ $(=\sqrt{8/3} = 1.633)$ [$c/a = 1.59$ for α-Ti (*15*) and $c/a \sim 1.60$ for ε-Fe (*16*)], elastic wave velocities are lower along the c axis than perpendicular to it. The anisotropy of the compressional wave in ε-Fe is ~4% (*16*).

Under the high-temperature conditions in the inner core, metals are paramagnetic. Paramagnetic susceptibility comes from two sources, namely spin paramagnetism and orbital paramagnetism (*17*). Ducastelle and Cyrot-Lackmann (*18*) showed that the anisotropy of paramagnetic susceptibility in hcp transition metals is controlled by two parameters, namely

$$\Delta\chi/\langle\chi\rangle = A\delta \qquad (1)$$

where $\Delta\chi = \chi_{\parallel} - \chi_{\perp}$ ($\chi_{\parallel}$ is the susceptibility parallel to the c axis and $\chi_{\perp}$ is the susceptibility perpendicular to the c axis), $\langle\chi\rangle$ is the average susceptibility, δ is equal to $[(c/a) - (c/a)_0]/(c/a)_0$, and A is a coefficient that depends on the number of d electrons. Volkenshtein *et al.* (*14*) found that the anisotropy of susceptibility in hcp transition metals has a correlation with the number of d electrons for a similar c/a, which suggests an important contribution from orbital paramagnetism. For materials with $\delta < 0$, $\Delta\chi$ is greater than 0 in hcp transition metals with an even number of d electrons (α-Ti, Hf, and Zr), but $\Delta\chi$ is less than 0 in hcp transition metals with an odd number of d electrons (Y, Ru, and Re) (Fig. 1). Iron has six d electrons ($3d^6$) and $c/a \sim 1.6$ for ε-Fe ($\delta < 0$). Therefore, the nature of paramagnetic susceptibility of ε-Fe will be similar to that of α-Ti, Hf, and Zr, namely $\Delta\chi > 0$. Volkenshtein *et al.* (*14*) also noticed that anisotropy in paramagnetic susceptibility decreases with temperature and vanishes near the melting temperature (Fig. 1). The temperatures in the Earth's core are highly uncertain, but I assume that the melting temperature of the outer core is significantly lower than that of the inner core because of the presence of light elements in the outer core (*1, 19*). Thus, the temperature at the outer-inner core boundary will be significantly lower than the melting temperature of pure iron, although a quantitative estimate is difficult. On the basis of the experimental results on α-Ti, Hf, and Zr, I estimate the anisotropy in paramagnetic susceptibility in ε-Fe at the inner core conditions to be $\sim 10^{-4}$ SI units (*20*).

When a magnetically anisotropic material is subject to a magnetic field, it will rotate in a way that will reduce the energy of the system. In the case of paramagnetism ($\chi > 0$), a material will tend to orient in such a way that the orientation with maximum susceptibility will be parallel to the orientation of the magnetic field. Lattice preferred orientation (texturing) due to this mechanism has been used to form polycrystalline materials with strong preferred orientation (magnetic annealing) (*21, 22*). In particular, de Rango *et al.* (*22*) demonstrated a strong preferred orientation of $YBa_2Cu_3O_7$ as a result of solidification from the melt with the presence of a magnetic field, a situation similar to the inner-outer core boundary of the Earth.

I propose that the solidification at the inner-outer core boundary in the presence of a magnetic field will result in a preferred orientation of Fe similar to that in the case of $YBa_2Cu_3O_7$. The critical parameter to control the preferred orientation in this case is the ratio, β, of anisotropic energy ΔE to the thermal energy kT (*22*)

$$\beta = \Delta E/kT = (1/2)\mu_0 \Delta\chi V H^2/kT \qquad (2)$$

where μ_0 is magnetic permeability of the vacuum [$4\pi \times 10^{-7}$ (H m^{-1})], V is the volume of the solid particle, H is the strength of the magnetic field, T is the temperature, and k is the Boltzmann constant (*23*). The parameter β must be significantly larger than 1 for a significant anisotropy to develop (*23*). Figure 2 shows the conditions at which this mechanism is effective as a function of grain size and the strength of magnetic field. It is seen that for a given anisotropy of paramagnetic susceptibility, a significant preferred orientation will be formed when both grain size and the magnitude of magnetic field are sufficiently large. A current estimate of the strength of the magnetic field in the core ranges from $\sim 10^{-3}$ to $\sim 10^{-2}$ T (*24*). For this range of field strength, significant preferred orientation will be formed if the grain size is larger than ~10 μm. Considering the slow cooling rate of the core, the grain size of freezing Fe should certainly be larger than ~10 μm

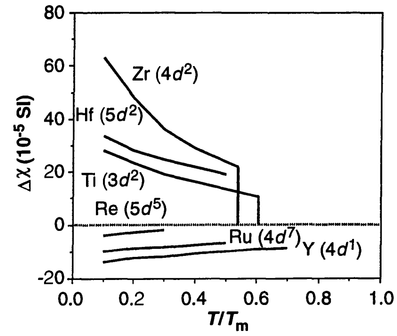

Fig. 1. Anisotropy of paramagnetic susceptibility in some hcp transition metals as a function of temperature (*14*) (T, temperature; T_m, melting temperature). Symbols in parentheses indicate the configuration of d electrons ($4d^2$ means two electrons in the $4d$ orbit, for example). Anisotropy in α-Ti and Zr vanishes at high temperatures because of the phase transition to bcc structure.

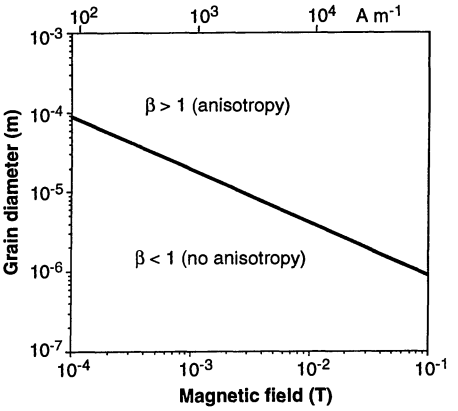

Fig. 2. The dependence of β (the ratio of anisotropic energy to thermal energy) on the magnetic field strength and grain size. When β is significantly larger than 1, the effect of anisotropy will dominate over the randomizing effect of thermal fluctuation, and a significant preferred orientation will result. For a reasonable range of magnetic field strength for the Earth's core (10^{-3} to 10^{-2} T), significant magnetic field–induced anisotropy will be formed if the size of crystallizing grains is larger than ~10 μm.

(*25*), and a strong lattice preferred orientation (LPO) will be expected.

An interesting consequence of this mechanism is that the LPO and the resultant seismic anisotropy will reflect the geometry (and strength) of the magnetic field. Two contrasting models of the geodynamo have been proposed (*24*): one with a strong toroidal field and the other with a weak toroidal field (*26*). Testing these models has been difficult because the toroidal field in the core is not directly observable. My model, if it is applicable, provides a useful constraint on the geometry of the magnetic field in the core and hence the model of the geodynamo (*27*). For a strong toroidal field model, the *c* axis of ϵ-Fe will be perpendicular to the rotation axis and the compressional wave velocity will be the fastest along the rotation axis. In contrast, for a weak field model the magnetic field in the core will be dominated by the poloidal field, and hence the compressional wave velocity will be the slowest along the rotation axis (Fig. 3). Therefore, the observed seismic anisotropy (the compressional wave velocity is the fastest along the rotation axis) supports the strong field model but not the weak field model of the geodynamo.

In more detail, some layering in anisotropic structure might occur if the inner core is convecting. The deformation mechanism of the inner core is most likely diffusion or superplastic creep, which will destroy the preferred orientation (*6*). Therefore, strong anisotropy will be observed mainly for the outer portion of the inner core. There is some evidence that anisotropy is stronger in the outer portions of the inner core than in the inner portions (*28*), which is consistent with my model.

A large uncertainty in my model is the assumption that hcp Fe is the dominant phase of the inner core. The presence of ϵ-Fe in the Earth's inner core has recently been questioned on the basis of high-pressure studies (*11*). However, the difficulties raised against convection-induced LPO apply to most of the possible phases of Fe (*5*). My model is largely free from these difficulties (*29*) but requires that the dominant phase of the inner core be noncubic Fe. Thus, although this model favors the noncubic structure of Fe in the inner core, further studies on the phase diagrams of Fe and their magnetic and elastic properties are needed to settle the issue. Finally, my model for seismic anisotropy will apply also to the outer core if the outer core has a significant amount of solid particles (*30*).

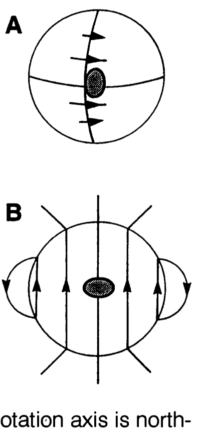

Fig. 3. Schematic diagrams showing the geometry of the magnetic field and the predicted anisotropy of compressional wave velocities in the inner core (magnetic field lines are indicated by the thin lines with arrows, and the anisotropic compressional wave velocities are shown by the ellipsoids). The anisotropic magnetic susceptibility and elasticity relevant to ϵ-Fe are assumed. The rotation axis is north-south. (**A**) Toroidal field. (**B**) Poloidal field. The seismological observations (the fast direction parallel to the rotation axis) are consistent with the dominance of the toroidal field in the core, which supports a strong field model of the geodynamo.

REFERENCES AND NOTES

1. A. P. Jephcoat and P. Olson, *Nature* **325**, 332 (1987); R. Jeanloz, *Annu. Rev. Earth Planet. Sci.* **18**, 357 (1990).
2. Anisotropy of the inner core has been inferred both from the analysis of the splitting of peaks of free oscillation of the Earth [J. H. Woodhouse, D. Giardini, X.-D. Li, *Geophys. Res. Lett.* **13**, 1549 (1986)] and from travel time anomalies of body waves [A. Morelli, A. M. Dziewonski, J. H. Woodhouse, *Geophys. Res. Lett.* **13**, 1545 (1986)] (*28*).
3. R. Jeanloz and H.-R. Wenk, *Geophys. Res. Lett.* **15**, 72 (1988).
4. S. Karato, in *High Pressure Research in Mineral Physics*, M. H. Manghnani and Y. Syono, Eds. (American Geophysical Union, Washington, DC, 1987), pp. 455–471; A. Nicolas and N. I. Christensen, in *Composition, Structure and Dynamics of the Lithosphere/Asthenosphere System*, K. Fuchs and C. Froidevaux, Eds. (American Geophysical Union, Washington, DC, 1987), pp. 111–123.
5. H. J. Frost and M. F. Ashby, *Deformation Mechanism Maps* (Pergamon, Oxford, 1982).
6. J. W. Edington, K. N. Melton, C. P. Cutler, *Prog. Mater. Sci.* **21**, 61 (1976); S. Karato, *Phys. Earth Planet. Inter.* **51**, 107 (1988).
7. The content of radioactive elements in the Fe meteorites [$<3 \times 10^{-16}$ W/kg] is much smaller than that in stony meteorites ($\sim 6 \times 10^{-12}$ W/kg) (*31*), which implies that the heat generation in the core that is a result of radioactive elements will be significantly lower than that in the mantle or crust. However, there is some evidence that the solubility of K in Fe might increase significantly with pressure (*32*), in which case the heat production in the core might be higher than that estimated from the radiogenic elements in the Fe meteorites.
8. A comparison of the density of the core with laboratory measurements indicates that a significant amount of light elements is present in the core, the outer core being more enriched with light elements than the inner core (*33*). F. D. Stacey (*31*) argued that the outer portion of the inner core might contain more of the light elements than the inner portion of the inner core through the growth process of the inner core by solidification from the outer core.
9. The degree to which this stabilization effect works may be measured by a nondimensional number Q [S. Chandrasekhar, *Hydrodynamic and Hydromagnetic Stability* (Oxford Univ. Press, Oxford, 1961)], defined as $Q = B^2\sigma R^2/\nu\rho$, where B is the magnetic flux, σ is the electrical conductivity, R is the radius of the inner core, ρ is the density, and ν is the kinematic viscosity. Using reasonable numbers for the measurement of each of these properties (Table 1), one gets $Q \sim 10^2$ to 10^4, which implies a significant stabilizing effect.
10. Jeanloz and Wenk (*3*) argued that the data of Jephcoat *et al.* (*16*) suggest a significant increase in elastic anisotropy with pressure. However, such an effect, to be seen in the curvature of a plot of *c*/*a* versus pressure, is not clearly observed in the latter's original data.
11. The structure of Fe at the inner core has been controversial. In addition to the hcp structure that has commonly been assumed (*1*), alternative structures have also been suggested on the basis of experimental and theoretical studies. They include cubic structures such as fcc [F. Birch, *Geophys. J. R. Astron. Soc.* **29**, 373 (1972); O. L. Anderson, *Philos. Trans. R. Soc. London Ser. A* **306**, 21 (1982); M. Brown and R. McQueen, *J. Geophys. Res.* **91**, 7485 (1986); Q. Williams, E. Knittle, R. Jeanloz, *ibid.* **96**, 2171 (1991)] or bcc [M. Ross, D. Young, R. Grover, *J. Geophys. Res.* **95**, 21713 (1990)] or a tetragonal structure [L. Stixrude and R. E. Cohen, in *Physics of Iron*, Proceedings of the Association for the International Advancement of High Pressure meeting at Colorado Springs, CO, 28 June to 2 July 1993, O. L. Anderson, Ed. (Lawrence Livermore National Laboratory, Livermore, CA, 1993), pp. 65–68; D. M. Sherman, *ibid.*, pp. 53–56]. Essential features of the following argument will apply for any noncubic structures, although specific predictions on the nature of anisotropy will depend on the assumed structure.
12. Magnetic susceptibility is a second-rank tensor and hence will be isotropic for the cubic structure. Elastic constant is a fourth-rank tensor and hence can be anisotropic even for a cubic structure. Therefore, Fe with a bcc or an fcc structure could cause seismic anisotropy, but deformation due to dislocation creep is unlikely for bcc or fcc metals at supposedly low stress conditions in the inner core (*5*).
13. E. W. Collings and J. C. Ho, *Phys. Rev. B* **2**, 235 (1970).
14. M. V. Volkenshtein, E. V. Galoshina, T. N. Panikovskaya, *Sov. Phys. JETP* **40**, 730 (1975).
15. H.-R. Wenk, T. Takeshita, R. Jeanloz, G. C. Johnson, *Geophys. Res. Lett.* **15**, 76 (1988).
16. A. P. Jephcoat, H.-K. Mao, P. M. Bell, *J. Geophys. Res.* **91**, 4677 (1986).
17. C. Kittel, *Introduction to Solid State Physics* (Wiley, New York, ed. 6, 1986).
18. F. Ducastelle and F. Cyrot-Lackmann, *J. Phys. (Paris)* **C1**, 536 (1971).
19. R. Boehler, *Nature* **363**, 534 (1993).
20. The precise value of $\Delta\chi$ is not very important for a qualitative discussion here, although the determination of $\Delta\chi$ for Fe stable at inner core conditions will be important in more quantitative studies.
21. A. Goetz, *Phys. Rev.* **35**, 193 (1930); W. W. Mullins, *Acta Metall.* **4**, 421 (1956); D. E. Farrell *et al.*, *Phys. Rev. B* **36**, 4025 (1987).
22. P. de Rango *et al.*, *Nature* **349**, 770 (1991).
23. My model does not provide a quantitative estimate of preferred orientation. However, the strength of preferred orientation due to recrystallization or crystallization is generally significantly larger than that due to deformation [G. Gottstein and H. Mecking, in *Preferred Orientation in Deformed Metals and Rocks: An Introduction to Modern Texture Analysis*, H.-R. Wenk, Ed. (Academic Press, New York, 1985), pp. 183–218], and a strong preferred orientation is observed in magnetically annealed materials (*21*, *22*).
24. R. T. Merrill and M. W. McElhinny, *The Earth's Magnetic Field: Its History, Origin and Planetary Perspective* (Academic Press, New York, 1983).
25. The grain size is determined by the kinetics of nucleation and growth and will be large when the cooling rate is slow [B. Chalmers, *Principles of Solidification* (Wiley, New York, 1964)]. Observations on some metallic systems indicate that the grain size of the slowly cooling Earth's inner core should be larger than ~1 cm [B. Cantor and R. D. Doherty, *Acta Metall.* **27**, 33 (1979); M. Rappaz and Ch.-A. Gandin, *ibid.* **41**, 345 (1993)].
26. A model with a strong toroidal field assumes that the Coriolis force in the liquid core is balanced with the Lorentz force (magnetostrophic balance), and a model with a weak field assumes that the Coriolis force is balanced with the pressure gradient (geostrophic balance).

]

27. The preferred orientation of inner core materials will be controlled by the magnetic field near the inner-outer core boundary, which may be somewhat different from the magnetic field in the bulk of the outer core, but the difference is not very large for a reasonable range of parameters [R. Hollerbach and C. A. Jones, *Phys. Earth Planet. Inter.* **75**, 317 (1993)].
28. K. C. Creager, *Nature* **356**, 309 (1992); X. D. Song and D. V. Helmberger, *Geophys. Res. Lett.*, in press.
29. An alternative mechanism for preferred orientation without deformation is proposed by M. Kumazawa [discussed in (*31*), pp. 210–211)], where differential stress due to the anisotropic growth rate of the inner core is considered to cause a preferred orientation. This process is highly unlikely to be important, however, because the anisotropic energy caused by this process is several orders of magnitude smaller than the magnetic anisotropic energy. Also, there is no experimental data to support the notion of stress-induced preferred orientation (*6*).
30. D. R. Fearn, D. E. Loper, and P. H. Roberts [*Nature* **292**, 232 (1981)] proposed that a layer of a solid-liquid mixed region (mushy layer) might extend deep into the inner core. Such a mushy layer might also extend into the outer core, and in this case my model of seismic anisotropy will also apply there.
31. F. D. Stacey, *Physics of the Earth* (Brookfield Press, Queensland, ed. 3, 1992).
32. M. S. T. Bukowinski, *Geophys. Res. Lett.* **3**, 491 (1976); E. Ito *et al.*, *ibid.* **20**, 1651 (1993).
33. A. E. Ringwood, *Proc. R. Soc. London Ser. A* **395**, 1 (1984).

34. I am grateful to S. K. Banerjee, B. Moskowitz, and D. A. Yuen for discussion, to O. L. Anderson and F. D. Stacey for constructive comments, and to X. D. Song for sending me a copy of their paper before publication.

13 July 1993; accepted 7 October 1993

Adhesive Electroless Metallization of Fluoropolymeric Substrates

Terrence G. Vargo, Joseph A. Gardella Jr.,* Jeffrey M. Calvert,*
Mu-San Chen

A process for producing patterned metal deposits on fluoropolymeric substrates is described. A metal ion–chelating organosilane is chemisorbed by self-assembly onto a fluoropolymer surface after radio-frequency glow discharge plasma surface hydroxylation. Positional modulation of the surface hydrophobicity is illustrated by wetting. The silane covalently binds an aqueous palladium catalyst and subsequent electroless deposition yields homogeneous or patterned metal deposits that exhibit excellent adhesion to the fluoropolymer.

Fluoropolymers such as poly(tetrafluoroethylene) (PTFE) and Teflon are of considerable technological importance because the low surface energy and stable C–F bonds provide surfaces that are inert to most solvents and chemicals and that prevent the adhesion of most chemical and biological materials (*1*). The low dielectric constants of fluoropolymers make them particularly attractive as dielectric layers for microelectronic applications (*2, 3*). However, for certain applications in which it is desirable to use fluoropolymers as a substrate, relatively few chemical pathways exist for the stable attachment of materials to the fluorinated surfaces. In this report, we apply the separately developed concepts of fluoropolymer surface hydroxylation (*4*) and subsequent organosilane functionalization (*5–8*) with ligand-based electroless deposition (*9–13*); the combination of these techniques yields a simple, effective method for producing adherent metal deposits on fluoropolymers, either homogeneously or in a pattern.

Approaches for promoting adhesive bonding of various materials, including metals, to fluoropolymer surfaces typically use harsh chemical reagents (highly reducing alkalies, such as sodium naphthalide) or require complex sputtering or ion beam bombardment processes (*2, 3*). A recently reported process (*14*) involves cross-linking of PTFE with x-rays followed by chemical etching and then vapor deposition of Cu by decomposition of an organocopper reagent. These methods are often difficult to use, may be environmentally problematic, and can adversely affect the chemical and morphological characteristics of the surface.

We have recently shown that fluoropolymers can be functionalized by chemisorption of organosilane reagents to plasma-treated fluoropolymer surfaces (*4–8*). Radio-frequency glow discharge (RFGD) treatment of the fluoropolymer surface using a novel gas-liquid mixture (*4*) partially defluorinates the surface with simultaneous addition of hydroxyl functionalities. An important aspect of this plasma treatment is that the surface is modified without inducing significant roughening. The hydroxylated surface exhibits a reactivity similar to that of Si–OH groups on silicon oxide surfaces and can be reacted with organosilane reagents to covalently immobilize various desired functionalities on the fluoropolymer surface (*5–8*). It has also been shown that use of a mechanical mask can restrict plasma treatment to particular regions of the surface; subsequent attachment of the organosilane occurs only in the areas exposed to the plasma. Such patterned aminoalkylsilane-fluoropolymer surfaces have been successfully used as chemical templates for the selective attachment and growth of neurons (*7, 8*).

We have also shown that selective, adhesive metallization of a wide range of nonfluorinated substrates to submicrometer resolution can be accomplished by electroless deposition (*11–13, 15–17*). Surfaces functionalized with self-assembled monolayer (SAM) films of ligand-bearing organosilanes covalently bind a Pd catalyst (*10, 18*) from aqueous solution and are then metallized by immersion in an aqueous electroless deposition bath. As shown below, fluoropolymer surface modification and ligand-based electroless deposition can be combined to yield patterned, adhesive metallization on these substrates.

It has been demonstrated that wetting is an extremely effective technique for imaging a surface that has patterns of functional groups with differing surface energies (*19, 20*). Drops of liquid are placed on the patterned surface and observed by optical microscopy. Outward curvature of the drop indicates the extent to which the liquid spreads on the surface; inward curvature indicates that the liquid does not appreciably wet the surface. We used this approach to visualize the increased density of hydroxyl groups in selected surface regions of a plasma-treated fluoropolymer. Poly(hexa-

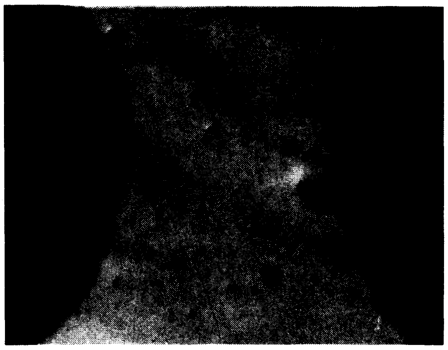

Fig. 1. Optical micrographs of sessile drops of water (left) and CH_3OH (right) placed on a patterned, plasma-treated FEP surface. We prepared the patterned surface by placing a Ni mask having 70-μm-wide lines separated by 150-μm-wide open regions in mechanical contact with a free-standing FEP film 50 μm thick. Modification was performed in an RFGD plasma with a radio-frequency power density of 1 W/ml at a pressure of 0.1 torr in a H_2-CH_3OH mixture for 15 s.

T. G. Vargo and J. A. Gardella Jr., Department of Chemistry, State University of New York, Buffalo, NY 14214.
J. M. Calvert, Center for Bio/Molecular Science and Engineering (Code 6900), Naval Research Laboratory, Washington, DC 20375.
M.-S. Chen, Geo-Centers, Inc., Fort Washington, MD 20744.

*To whom correspondence should be addressed.